出國報告（出國類別：參加國際研討會）

2015 International Conference on Applied System Innovation 國際研討會)

服務機關：國立虎尾科技大學光電工程系
姓名職稱：劉代山 教授
派赴國家：日本
出國期間：2015 年 5 月 21 日至 5 月 26 日
報告日期：2015 年 09 月 04 日

摘要

　　本人此次參與日本大阪所舉行 2015 International Conference on Applied System Innovation 國際研討會，除擔任大會 Program Committee 委員會委員，並在會議中發表一篇文章著作外，亦擔任會議主持人(session A2)，本次會議領域包含有材料科學與工程、通訊科學與工程、電腦科學與資訊技術、計算科學與工程、電子與電機工程、機械與自動化工程、綠能技術與建築工程、工業設計與設計原理及應用數學等相關研究領域，會議文章發表方式包含邀請報告、口頭報告與海報張貼等，分為 26 個子會議共 420 篇文章，此次會議除了主持會議與發表文章外，更提供本人與相關領域傑出學者及專家學習與意見交流的機會，對於提升本人學術研究能量與國際視野助益甚大。

目　次

目的

　　2015 International Conference on Applied System Innovation 國際研討會舉辦地點在日本大阪市，本次參加學者除了有台灣相當知名的學者教授(陳朝光教授、李清庭教授、張守進教授)，另有日本、捷克、羅馬尼亞及泰國等國家的學者一同參與本研討會。大會並特別邀請由張俊彥教授以及 Sakai 博士分別進行主題演講與邀請演講。各位報告者皆簡報目前的研究內容成果，內容豐富充實，本人亦有發表一篇文章。藉由此次會議不僅有助於提升本實驗室的在研發能量上能見度，藉由與與會專家學者的學術交流，更可以開拓本人的視野並開啟與先進團隊合作研究的契機。

過程

　　本人於5月21日由台灣桃園國際機場搭乘華航班機，於日本當地時間晚上約6點20分抵達日本大阪關西國際機場，但由於關西機場出關作業緩慢遲至晚間約9點方完成通過程序，幸好研討會主辦單位貼心安排與會專家學者搭乘專車前往會議地點之南淡路島皇家飯店，因此，儘管抵達飯店下榻時已是深夜11時許，本人稍事休息並整理行李後仍興致勃勃的研讀研討會資料。

　　5月22日一大早起床用完早餐並打理完畢後，本人旋即至研討會櫃檯辦理會議註冊手續，並熟悉及參觀研討會各討論室地點與環境，以為即將到來的海報張貼與會議主持工作預做準備，接著，依循大會所提供的會議手冊資料，於上午九時許參與研討會開幕儀式，儀式當中首先由會議主席－台灣成功大學張守進教授致詞並宣讀歡迎辭，並由台灣知識創新學會會長－閔庭輝教授致詞並頒發感謝狀，緊接著本人參加由大會精心邀請的主題演講與邀請演講，其中，主題演講係由台灣師範大學－張俊彥教授演講 "The ECNG interdisciplinary research: education, cognition, neuroscience, and gene"，其內容針對目前各國教育制度與方法的僵化現象，進行廣泛的探討並提出改善計畫，嘗試以翻轉式教學方式激發研究生與學生的創意與研發能量，該領域雖與本人工程研究內容有較大的差異，但所使用的教育方法與激發研究潛能想法，提供本人對於培育工程科技專業人才與前瞻研發能量有相當大的啟發，張教授更利用自身經歷與周邊事務，深入淺出地描述該創新方式的成效與實績，另本人印象深刻。緊接著，大會安排由日本 The National Institute of Advanced Industrial Science and Technology 首席研究員 Tetsuo Sakai 博士，演講"Development of advanced battery materials and battery design for improving safety and heat-resistance on xEV and energy storage systems"，Dr. Tetsuo Sakai 擁有超過 300 項專利並發表超過 300 篇學術文章，其主要的報告內容是關於開發新式的能源材料及電池設計，以提升電池的效能，作為目前提供汽車能源，且為了增加其應用的效能，其電池的儲存容量及其體積與重量也是目前電池是否能被廣泛的應用於汽車產業之中。隨著目前的電池開發發展趨勢而言，於未來幾年中，將大有機會把原本提供汽車能源的時由改成利用電力直接驅動，以解決目前能源的危機及改善環境污染。聽完 Sakai 博士演講後，除了感受到日本人在研究與創新方面的嚴謹與執著外，其研究成果除了更能啟發本人對於能源的進一步認識，對於應用於汽車工業上的發展與未來展望也有更清楚的了解。

　　當天下午本人與楊勝州教授教授一同擔任材料科學與工程領域第二場會議報告的會議主

席，該場次共有 "ZnO Nanorod Arrays Fabricated by Hydrothermal Method using Different Thickness of Seed Layer for Applications in Hybrid Photovoltaic Cells"、"Study of the Formation and Switching Behavior of 360 Degree Domain Wall in Permalloy Thin Film Ring"、"Investigation on the Generation of Multiple 360 degree Domain Wall through Different Shapes of Generators and Stoppers"、"Grid Task Scheduling Using Adaptive Search Control Particle Swarm Optimization"、"Epitaxial growth of GaN on ZnO micro-rod by plasma-assisted molecular beam epitaxy"、"A TRIZ-based Approach to Investigating Evolutionary Trends and Contradiction Analysis for Product Design" 以及 "The Influences of Drawing with Graphics Software on Children's Cognitive" 等 7 篇文章發表，令人印象深刻的是其中一篇由日本研究團隊發表利用水熱法成長 ZnO 奈米柱的研究內容，該文章係探討在不同晶種層厚度下沉積 ZnO 奈米柱，並將其應用於混合性光伏元件的特性量測結果，研究中首先利用 XRD、SEM 等設備分析奈米柱的結構特性，最終，將最佳的 ZnO 奈米柱應用於 hybrid photovoltaic cells 時，其能量轉換效率可以達 1.02%。

5 月 23 日到達研討會現場，除了與各界專家學者討論研究成果與心得外，亦聽取一些與研發相關的論文內容發表，其中，另人印象較深刻的是論文題目為"Fabrication and characterization of a-IGZO thin-film-transistors with passivation layers"的研究報告，薄膜電晶體是主動式平面顯示器中的一個重要的元件，薄膜電晶體能單一控制畫素的開關元件，目前製作薄膜電晶體所選用的材料有非晶矽、低溫多晶矽及氧化銦鎵鋅等。非晶的氧化銦鎵鋅薄膜電晶體與非晶矽及低溫多晶矽薄膜電晶體相較而言，其具有較高的等效載子移動率，所以目前有許多相關的研究提出關於此材料的導電物理機制。講者所提出的研究內容是利用磁控式濺鍍系統製備氧化銦鎵鋅薄膜及二氧化矽薄膜分別作為薄膜電晶體的通道層與閘極絕緣層，研究在長時間水氣及氧氣環境下，氧化銦鎵鋅薄膜電晶體的穩定特性。我們實驗室亦有進行利用磁控式射頻共濺鍍方式製作氧化銦鎵鋅薄膜電晶體，未來我們會將其應用於軟板製作。

5 月 24 日抵達研討會現場，除了與熟識的研究同仁閒話家常並寒暄問暖外，也聽到了一些有趣的論文題目發表，其中，論文題目為 "The influences of Copper doping concentrations on the properties of ZnO films by RF magnetron sputtering" 尤其今本人感到興趣，作者利用磁控濺鍍系統、在 Corning 7059 玻璃上沉積具有原子濃度為 2%至 10%的銅摻雜氧化鋅薄膜，利用 XRD、XPS、穿透率以及電特性量測結果，觀察不同 Cu 濃度摻雜 ZnO 薄膜的光、電以及材料特性變化，該團隊研究結果顯示，隨著 Cu0 摻雜濃度上升薄膜中的氧缺陷會隨之增加，且結構中的 ZnO(103)晶面成長取向也會隨之增強，此外，由於 Cu 摻雜在 ZnO 薄膜中含量的增加，其穿透率也會有些微下降的趨勢，且電阻率由於薄膜結晶性劣化以及晶界增加，而有較顯著上升的現象，最終結果顯示，當氧化鋅薄膜中 Cu 原子摻雜濃度達 2%時，有最佳的光、電與材料特性。

5 月 25 日研討會進行到第四天，經過多天的相處，可以發現，許多來到此地的專家學者，

更能融入彼此暢所欲言，今天同樣吸取許多論文發表的研究精神與內容，其中，論文題目為 "Effect of Fe-doped" TiO2 photocatalysts on the degradation of acid orange 7"，與本人其中之一研究內容相關，因此格外吸引本人注意，作者係利用 Solid-reaction technology 製作 Fe 莫耳摻雜濃度為 2%的 TiO2 光觸媒材料，探討不同製程過程時所製備 Fe-TiO2 奈米粒子的粒徑大小、比表面積以及孔隙尺寸，對於 acid orange 7 的降解能力，結果顯示，在 100 ml 的 AO7 溶液中加入 0.1 g 的 Fe-TiO2 粒子，在 UV 光照射下其降解速率最高可達 88.7%。

5 月 26 日下午，本人懷著充實而滿足的心情，搭乘大會提供的巴士至日本大阪關西機場搭乘華航班機飛抵台灣桃園國際機場。

心得及建議

本次參加在日本大阪所舉行的 2015 International Conference on Applied System Innovation 國際研討會，除了有許多國外專家學者參加外，更有許多國內不同領域的知名學者與會，在開會期間除了可以與相關領域研究先進學習並討論研究成果外，藉由大會安排的各個專題與會議演講，更可以提供本人深入了解其他相關領域的研究內容與方向，提供本人進一步從事跨領域研究的動機與可行性，此外，大會精心安排的接送工具與行程，更可以讓本人在無後顧之憂的環境下，充分與與會學者專家先進進行深入的探討與學習，不僅有助於充實本人研究能量，更可以提供本人對於未來研究方向的啟發。

會議照片

大會開幕式：

邀請演講內容：

與發表論文海報合影

發表海報論文

研討會一隅
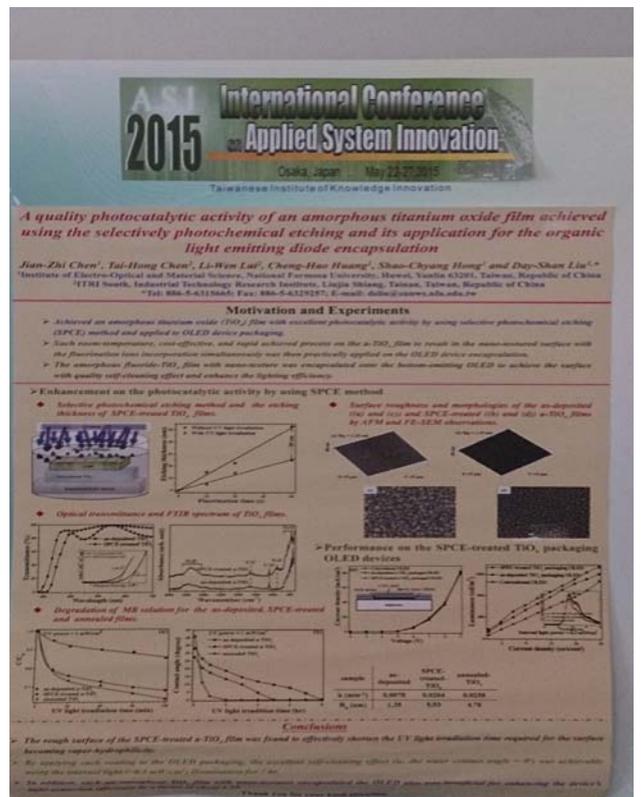
附錄：攜回資料名稱及封面
Proc. of 2015 International Conference on Applied System & Innovation

附錄：攜回資料名稱及封面

A quality photocatalytic activity of an amorphous titanium oxide film achieved using the selectively photochemical etching and its application for the organic light emitting diode encapsulation

Jian-Zhi Chen[1], Tai-Hong Chen[2], Li-Wen Lai[2], Cheng-Hao Huang[1], Shao-Chyang Hong[1], and Day-Shan Liu[1,a]

[1]Institute of Electro-Optical and Material Science, National Formosa University, Yunlin, Taiwan

[2]ITRI South, Industrial Technology Research Institute, Tainan, Taiwan

[a]dsliu@sunws.nfu.edu.tw

Abstract. In this study, a rapid, cost-effective, and room-temperature achieved selectively photochemical etching (SPCE) method was developed to improve the photocatalytic activity of a PECVD-deposited amorphous titanium oxide (a-TiO$_x$) film. The a-TiO$_x$ film treated by the SPCE method for only 60 sec. showed the photocatalytic activity comparable to that of a high-temperature prepared TiO$_x$ film with anatase structures. The mechanism responsible for the significant enhancement on the photocatalytic activity was ascribed to the formation of the nano-textures with the incorporating of fluorine ions on the surface as examined using AFM, FE-SEM, and XPS measurements. The SPCE-treated a-TiO$_x$ film was then applied to encapsulate the blue organic light emitting diode (OLED) to result in the surface with self-cleaning function. A super-hydrophilic surface (i.e. the water contact angle below 5°) was available after irradiating the device's light (~0.3 mW/cm^2 at 488 nm) for 5 hrs. In addition, the OLED encapsulated by the SPCE-treated a-TiO$_x$ film also was beneficial for the enhancing the light-extraction efficiency by a factor of 1.25 as a consequence of its notably nano-textured surface.

Microelectronic Engineering

A quality photocatalytic activity of an amorphous titanium oxide film achieved using the selectively photochemical etching and its application for the organic light emitting diode encapsulation

Jian-Zhi Chen [a], Tai-Hong Chen [b], Li-Wen Lai [b], Cheng-Hao Huang [a], Shao-Chyang Hong [a], Day-Shan Liu [a],*

[a] Institute of Electro-Optical and Materials Science, National Formosa University, Huwei, Yunlin 63201 Taiwan, ROC
[b] ITRI South, Industrial Technology Research Institute, Liujia Shiang, Tainan, Taiwan, ROC

ABSTRACT

In this study, a rapid, cost-effective, and room-temperature achieved selectively photochemical etching (SPCE) process was developed to improve the photocatalytic activity of a PECVD-deposited amorphous titanium oxide (a-TiO$_x$) film. The a-TiO$_x$ film treated by the SPCE process showed a photocatalytic activity comparable to that of a high-temperature prepared TiO$_x$ film. As examined from the surface roughness and morphologies, optical transmittance, and chemical bond configurations, the mechanism responsible for the significant enhancement on the photocatalytic activity was ascribed to the formation of the nano-textures with the increase in the surface acidity due to the incorporating of fluorine ions. The SPCE-treated a-TiO$_x$ film with the quality photocatalytic activity was then applied to encapsulate the blue organic light emitting diode (OLED) to result in the surface with self-cleaning function. A super-hydrophilic surface was available using the internal light irradiation. In addition, the OLED encapsulated by the SPCE-treated a-TiO$_x$ film also was beneficial for enhancing the light-extraction efficiency as a consequence of its notably nano-textured surface.

© 2015 Elsevier B.V. All rights reserved.

1. Introduction

Transparent titanium oxide (TiO$_x$) film possesses a high refractive index has been comprehensively used as an optical coating for several decades. Its excellent photocatalytic activity also has attracted significant attention as specific function, such as anti-bacterial, anti-pollution, decolourization, and deodorization, for the environmental purification, dye-sensitization, surface self-cleaning/antifogging, and biomedical engineering applications [1–4]. Since the TiO$_x$ film with anatase phase is the known structure that exhibited the best photocatalytic activity, most researchers are devoted to enhance its efficiency via increasing the film's specific surface area and/or retarding the recombination of the photo-generation electro-hole pair [5–9]. Unfortunately, the prepared temperature required for the crystallization of the TiO$_x$ film with anatase phase typical was too high to apply as a modification coating on the temperature-sensitive substrate or device packaging. Accordingly, low-temperature prepared hydro-oxygenated amorphous TiO$_x$ (a-TiO$_x$) film abundant in OH groups using plasma-enhanced chemical vapor deposition (PECVD) has became a promising candidate in substitution for the high-temperature obtained crystal-TiO$_x$ film. However, the photocatalytic activity of the PECVD-deposited a-TiO$_x$ film still was a grade inferior to that of the anatase TiO$_x$ film [10,11], revealing that more effort to enrich the surface activation of the PECVD-deposited a-TiO$_x$ film is needed. As quoted from the previous reports to modify the surface property of the a-TiO$_x$ film [12–14], we developed a room-temperature achieved two step process consisted of the selective pre-irradiation and the following fluorination etching to improve the film's photocatalytic activity [15]. Though the results demonstrated that the a-TiO$_x$ film modified by this two step process exhibited a quality photocatalytic activity comparable to the anatase-TiO$_x$ film, the selective pre-irradiation on the film for the sequential fluorination etching was too long (5 h) to realize the applications on the substrate modification or device packaging.

With the aim to simplify and shorten the above-mentioned two step process to realize its application on substrate modification and device packaging, a selectively photochemical etching (SPCE) process combined with the selective UV light irradiation and fluorination etching simultaneously was presented in this work. Such room-temperature, cost-effective, and rapid achieved process on the a-TiO$_x$ film to result in the nano-textured surface with the fluorination ions incorporation was then practically applied to the OLED device encapsulation. In addition to investigate the enhancement on the photocatalytic activity of the SPCE-treated a-TiO$_x$ film, the improvement on the photo-induced surface wettability using the external UV and internal blue light irradiation as well as the light extraction efficiency for the OLED device encapsulated by the SPCE-treated a-TiO$_x$ film also was measured and discussed.

* Corresponding author.
E-mail address: dsliu@sunws.nfu.edu.tw (D.-S. Liu).

2. Experimental

Hydro-oxygenated a-TiO$_x$ films with thickness of 200 nm were deposited onto silicon and glass substrates by PECVD using titanium tetraisopropoxide (Ti(OC$_3$H$_7$)$_4$, TTIP) and oxygen gas mixture. The titanium precursor was reservoired in a bubbling cylinder heated at 70 °C with the nitrogen carrier gas, and the gas line was heated to 100 °C to prevent condensation. The TTIP-oxygen gas mixture was sprayed through a showerhead array at the upper electrode, which was 50 mm away from the substrates' holder. The deposition pressure, rf power, and gas flow rate of TTIP/O$_2$ gas mixture were controlled at 40 Pa, 100 W, and 120/20 sccm, respectively. Then, the SPCE process was treated on these a-TiO$_x$ films by immersing these samples in a 0.5 vol.% dilute hydrofluoric acid (HF) solution and selectively irradiating by an UV lamp (TLD 10 W/08, Philips; centered at 365 nm with the intensity of 3 mW/cm^2) through a porous alumina anodic membrane (AAM) mask simultaneously. The UV light intensity and the acid concentration for achieving the SPCE process were designed to effectively activate the surface property to resist the concurrent etching process and thus result in the optimal selective fluorination etching. Fig. 1 illustrates a schematic configuration of this SPCE process. Another set of the as-deposited a-TiO$_x$ films were annealed at 500 °C for 30 min under oxygen ambient (hereafter denoted as annealed TiO$_x$) to cause the structural crystallization with anatase phase for comparing their photocatalytic activity. Eventually, the a-TiO$_x$ films with and without the SPCE treatment were respectively deposited onto the top-emission OLED devices which had been passivate by a 300 nm-thick SiON barrier film.

Film thickness of these fluorinated samples with and without the UV light irradiation was measured using a surface profile system. The surface roughness and morphologies were observed using the atomic force microscopy (AFM, DI-3100, Veeco) and a field emission scanning electron microscope (FE-SEM, JSM-6700F, JEOL), respectively. Optical transmittance was measured using an UV–Vis-NIR spectrophotometer (UVD 3500, Labomed, Inc.). The chemical bond states of these samples were examined by a Fourier transform infrared (FTIR) spectrometry (FT/IR-4100, JASCO). Photocatalytic activity of the a-TiO$_x$ films as well as the annealed TiO$_x$ film was determined from the decolorization of a methylene blue (MB) solution by an UV light irradiation at a constant intensity of 1 mW/cm^2. In addition, the associated photo-induced surface wettability to water drop also was conducted by the water contact angle meter. The current density–voltage (J–V) and luminance–current density (L–J) properties of the OLED devices encapsulated by these a-TiO$_x$ films were measured using a semiconductor parameter analyzer and an integrated sphere detector.

3. Results and discussion

Fig. 2 shows the etching thickness for the a-TiO$_x$ films immersed in the dilute HF solution with and without the UV light irradiation
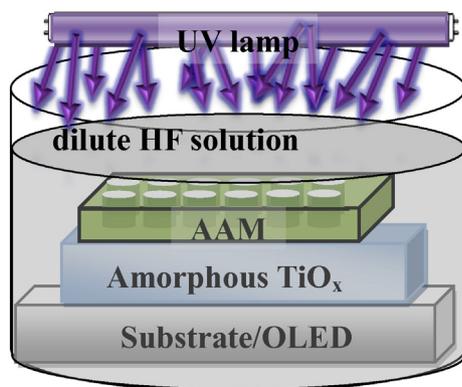
Fig. 1. Schematic configuration of the selectively photochemical etching process.
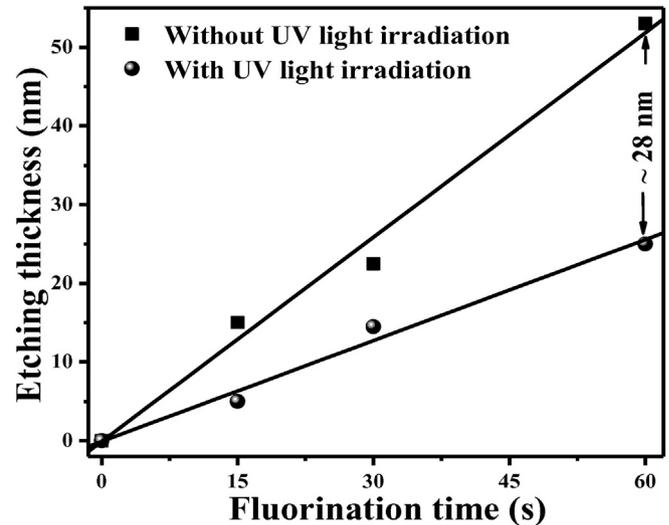
Fig. 2. Etching thickness for the a-TiO$_x$ films immersed in the dilute HF solution with and without simultaneously irradiating the UV light.

simultaneously. Since the electrons generated on the a-TiO$_x$ film by the UV light irradiation was prone to transform the surface Ti(IV) cation to Ti(III) state, as expressed in Eq. (1) [16], and thereby reduce the acidity of the etching solution [17,18], the etching thickness of the fluorinated a-TiO$_x$ film combined with the UV light irradiation thus was lower than that of the film only etched by the dilute HF solution.

$$e^- + Ti(IV)-OH \rightarrow Ti(III)-OH^- \hspace{2cm} (1)$$

Accordingly, the difference in the etching thickness between the fluorinated a-TiO$_x$ films with and without the UV light irradiation etched for 60 s was about 28 nm as indicated in Fig. 2. As the etching thickness on the a-TiO$_x$ film was apparently alleviated by incorporating with the UV light irradiation, a SPCE process combined with the selectively photocatalytic activation through a AAM mask with nano-sized porous (~20 nm) and the fluorination etching was carried out to roughen the film surface to enlarge its specific surface area. Fig. 3(a) and (b), respectively, illustrate the surface roughness of the as-deposited a-TiO$_x$ film and the SPCE-treated a-TiO$_x$ film for 60 s. It can be seen that large amounts of white and sharp protrusions distributed over the SPCE-treated a-TiO$_x$ film, resulting in its root–mean–square surface roughness, R$_q$, was significantly increased to 5.53 nm as compared to that of the as-deposited TiO$_x$ film (~1.35 nm). Fig. 3(c) and (d) further highlight the surface morphologies of the as-deposited and SPCE-treated a-TiO$_x$ films conducted from FE-SEM observations. The surface morphology of the as-deposited a-TiO$_x$ film exhibited densely and abnormally distributed particles with visible boundaries, while those particles distributed over the SPCE-treated a-TiO$_x$ film surface became separated with significant grooves. In addition, due to the fluorination etching on the areas of the a-TiO$_x$ film surface without the UV light irradiation were more drastic than the areas irradiated by UV light, the particles distributed over the SPCE-treated a-TiO$_x$ film almost had the same diameter of about 20 nm, a value very close to the porous size of the AAM mask. The optical transmittances of the as-deposited and SPCE-treated a-TiO$_x$ films are given in Fig. 4. The average transmittances in the visible wavelengths ranged from 400–700 nm for the as-deposited and SPCE-treated a-TiO$_x$ films were 88 and 96%, respectively. The increase in the average optical transmittance for the a-TiO$_x$ film treated by the SPCE process was both attributed to the thinner thickness as compared to the as-deposited a-TiO$_x$ film and the reduction in the reflectance due to its rougher surface [19]. In addition, the absorption onset of the SPCE-treated film also markedly shifted toward a shorter wavelength as compared to the untreated film. Accordingly, The
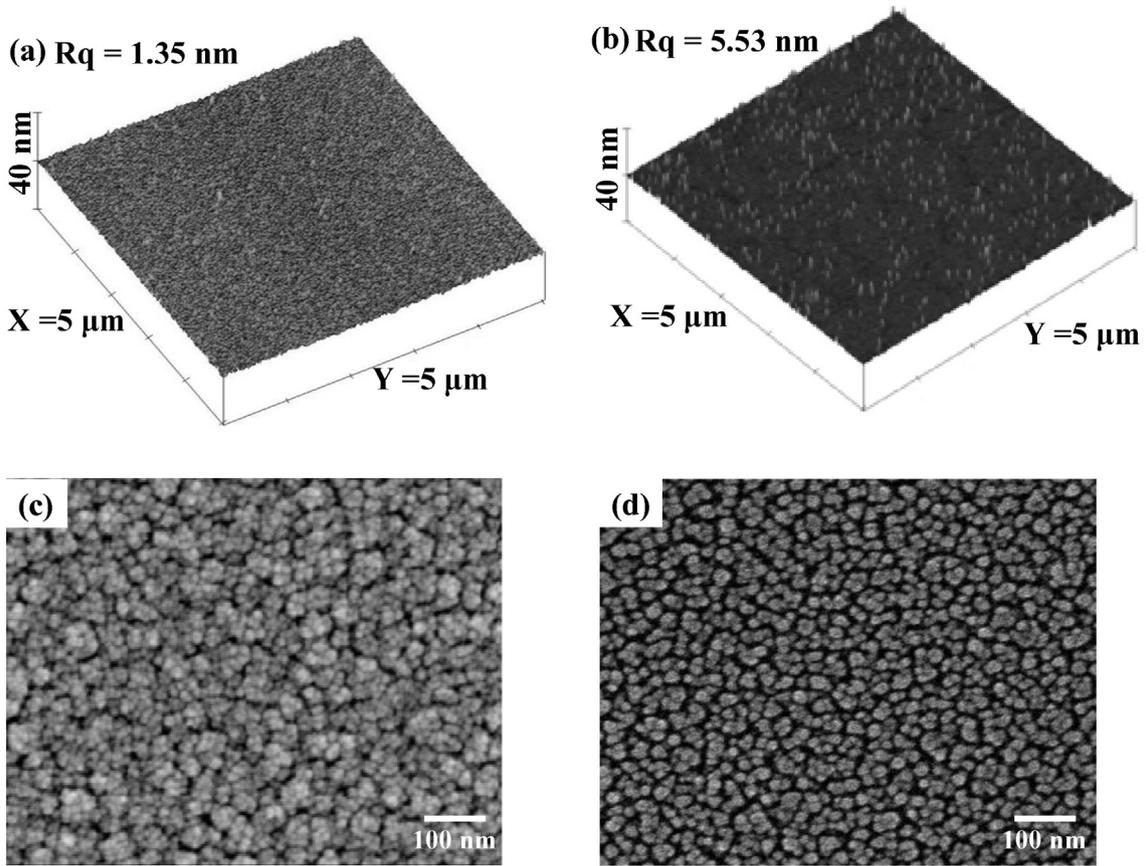
Fig. 3. Surface roughness and morphologies of the as-deposited ((a) and (c)) and the SPCE-treated ((b) and (d)) a-TiO$_x$ films by AFM and FE-SEM observations.

corresponded optical energy band gaps fitted from the plot of the $(\alpha h\nu)^{1/2}$ versus the photon energy (eV), as shown in the inset figure, for the as-deposited and SPCE-treated films were 3.36 and 3.39 eV, respectively. The particle quantization on the a-TiO$_x$ film surface treated by the SPCE process, as can be seen in Fig. 3(d), was responsible for the increase in the optical energy band gap. The chemical bond configurations appeared in the as-deposited and SPCE-treated a-TiO$_x$ films conducted by the FTIR measurements are given in Fig. 5. Both these films contained two feature signals around 400–800 cm^{-1} and 2800–3700 cm^{-1}, which are regarded as the stretching vibration mode of Ti–O bond and the surface hydroxyl (O–H) groups, respectively [11,20]. An additive signal approximately at 860 cm^{-1} associated with the Ti–F vibration mode can be seen in the FTIR spectrum of the SPCE-treated a-TiO$_x$ film, which shows evidence of the fluorine atoms incorporating into the film surface after the fluorination etching process. Because the fluorine is the most electronegative halogen element, in agreement with the reports [15,21], the surface acidity of the SPCE-treated a-TiO$_x$ film thus was increased and it also resulted in the enhancement and notable shift on the peak of the O–H bond from 3473 to 3373 cm^{-1}.
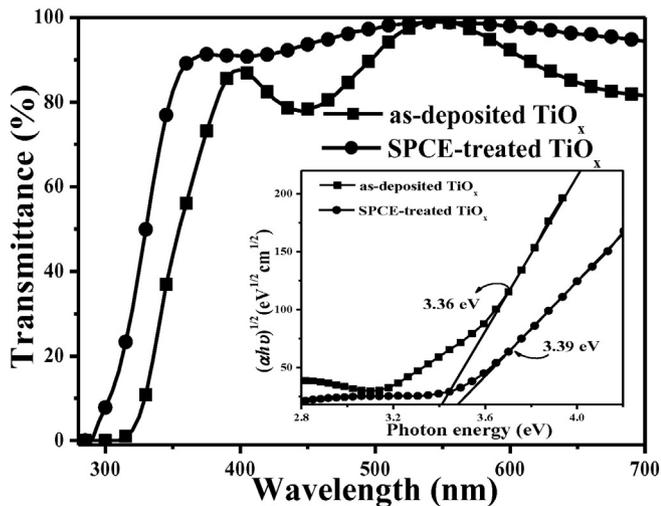
Fig. 4. Optical transmittances of the as-deposited and SPCE-treated a-TiO$_x$ films (the inset figure plots the corresponded $(\alpha h\nu)2$ versus the photon energy (eV)).
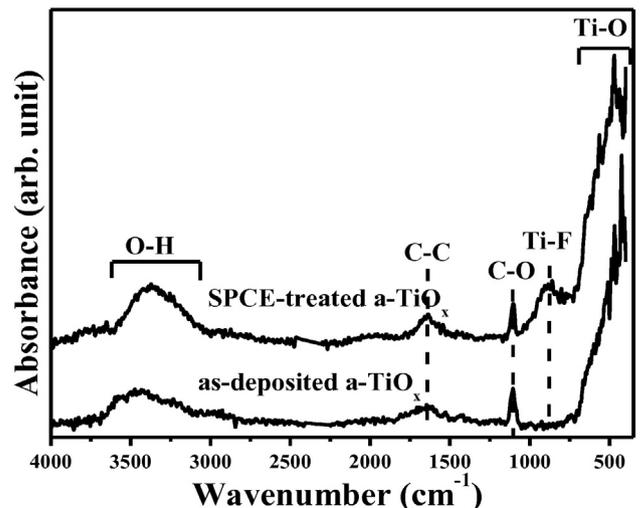
Fig. 5. FTIR spectra of the as-deposited and SPCE-treated a-TiO$_x$ films.

The UV-light induced photocatalytic degradation on the MB solution using the as-deposited and SPCE-treated a-TiO$_x$ films as well as using the annealed TiO$_x$ film is illustrated in Fig. 6(a). The roughened surface of the SPCE-treated a-TiO$_x$ film with the fluorine ions incorporation led to a high decomposition rate to MB solution as compared to the as-deposited a-TiO$_x$ film. The rate constant, k, which represents the film's photocatalytic activity, is determined from the photocatalytic degradation on the MB solution according to the following equation [21]:

$$\ln(C/C_0) = k\text{t} \tag{2}$$

where, C and C_0 are the concentration of the MB solution at UV light irradiation time of t = 0 and t, respectively. Table 1 summarized the rate constants and root–mean–square surface roughness of the as-deposited and SPCE-treated a-TiO$_x$ films as well as the annealed TiO$_x$ film. It can be seen that the photocatalytic activity of the SPCE-treated a-TiO$_x$ film to decompose the MB solution (the rate constant ~ 0.0204 min^{-1}) is significantly higher than that of the as-deposited film (~0.0078 min^{-1}) and only about 20% lower than that of the annealed TiO$_x$ film (0.0258 min^{-1}). Fig. 6(b) shows the photo-induced surface wettability to the water droplet of these three samples irradiated by UV light. Although the UV light irradiation time required for the contact angle to water droplet on the SPCE-treated a-TiO$_x$ film surface became 0° (5 h) was effectively shortened as compared to that of the as-deposited sample (8 h), the decrease in the water contact angel was slower than that of the annealed TiO$_x$ film (only irradiation

Table 1
Rate constant and root–mean–square surface roughness of the as-deposited and SPCE-treated a-TiO$_x$ films as well as the annealed TiO$_x$ film.

Samples	as-deposited a-TiO$_x$	SPCE-treated a-TiO$_x$	Annealed TiO$_x$
k (min^{-1})	0.0078	0.0204	0.0258
R$_q$ (nm)	1.35	5.53	4.78

for 2 h to became super-hydrophilic surface (i.e. water contact = 0°)). The reason responsible for the difference between the photocatalytic activity to decompose the MB solution and the photo-induced surface wettability to water droplet of the SPCE-treated a-TiO$_x$ film as compared to that of the annealed TiO$_x$ film was attributed to the fluorine ions that appeared on the film surface which preferred the reaction of cationic MB solution to water droplet [22,23]. Accordingly, the SPCE-treated a-TiO$_x$ film with the rough surface and fluorine ion incorporation exhibited notable photocatalytic degradation on the MB solution which was only slightly lower than that of the annealed TiO$_x$ film.

Fig. 7(a) shows the current density–voltage (J–V) curves of the OLED was only packaged by a 300 nm-thick SiON barrier layer (denoted as controlled OLED), and the OLEDs were additionally encapsulated by the as-deposited and SPCE-treated a-TiO$_x$ films (a schematic structure is shown in the inset figure). The nearly identical J–V characteristics indicate that the low-temperature achieved SPCE process on the
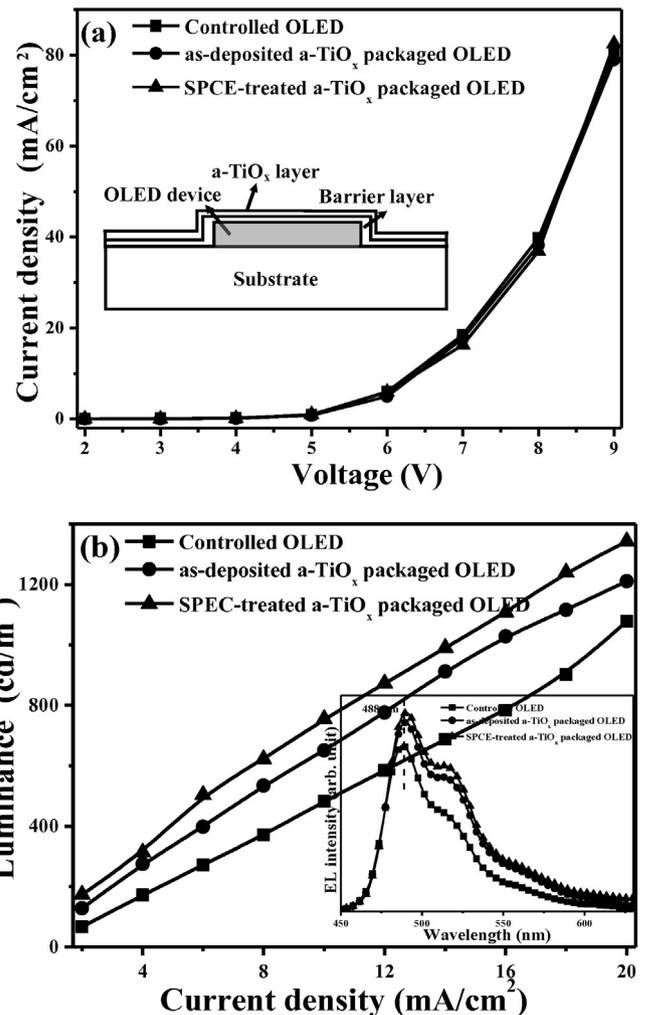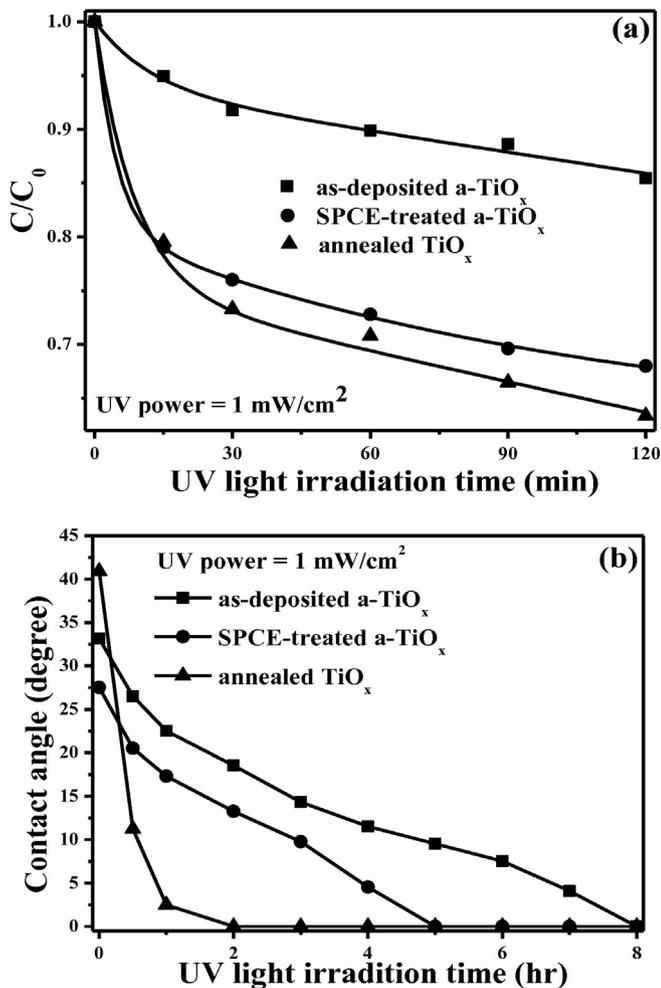
Fig. 6. (a) UV-light induced photocatalytic degradation on the MB solution and (b) photo-induced surface wettability to the water droplet using the as-deposited and SPCE-treated a-TiO$_x$ films as well as using the annealed TiO$_x$ film.

Fig. 7. (a) J–V and (b) L–J curves of the OLED only packaged by a 300 nm-thick SiON barrier layer (denote as controlled OLED), and the OLEDs additionally encapsulated by the as-deposited and SPCE-treated a-TiO$_x$ films (a schematic structure and the correspondent EL spectra are also shown in the inset figures).

controlled OLED device had little impact on the device performance. The corresponded luminance–current density (L–J) properties of these devices are illustrated in Fig. 7(b). The electroluminescence (EL) spectra at an injecting current density of 12 mA/cm² also are given in the inset figure. The emission peak of all these devices was located at 488 nm and the largest EL intensity was obtained from the OLED additionally encapsulated by the SPCE-treated a-TiO$_x$ film. Compared to the controlled OLED, the device additively encapsulated by the SPCE-treated a-TiO$_x$ film led to an increase in the output luminance of 25%. As quoted from our previous report [1], the enhancement on the light extraction efficiency of this OLED was attributed to the reduction of the Fresnel loss from the device that was encapsulated by the SPCE-treated a-TiO$_x$ film with the well-defined nano-textured surface. The photo-induced surface wettability of these OLEDs irradiated by an external UV light (1 mW/cm² at the wavelength of 365 nm) is shown in Fig. 8(a). Due to the surface property of the SiON barrier layer that was inactive to the UV light irradiation, the contact angle of the water droplet on the controlled OLED almost was unchanged after irradiating the external UV light for 8 h (from about 75° to 71°). By contrast, the water contact angles of the OLEDs additionally encapsulated by the as-deposited and SPCE-treated a-TiO$_x$ films became 0° after the samples irradiated for 8 and 6 h, respectively, revealing the achievement of the super-hydrophilicity on the devices' surface. Interestingly, although the blue light centered at 488 nm emitted from the OLED device was

hardly absorbed by the a-TiO$_x$ films, as shown in Fig. 4, the surface wettability of the devices additionally encapsulated by the as-deposited and SPCE-treated a-TiO$_x$ film could also be improved by the internal light illumination (0.3 mW/cm²), as shown in Fig. 8(b). Accordingly, an OLED device with truly self-cleaning function (ie. the contact angle of the water droplet is equal to 0°) after irradiating the internal light for 7 h was achievable by additionally encapsulating the SPCE-treated a-TiO$_x$ film.

4. Conclusions

A selective fluorination etching achieved by an UV light irradiation through AAM mask simultaneously to modify the surface property of the a-TiO$_x$ film was developed. This SPCE process on the a-TiO$_x$ film resulted in the well-defined nano-particles distributed over the film surface, and thereby led to a markedly increase in the surface roughness (5.53 nm) as compared to that of the as-deposited film (1.35 nm). In addition, the incorporation of the fluorine ions as evidence of the formation of the Ti–F chemical bond also implied the increase in the surface acidity. The rough surface of the SPCE-treated a-TiO$_x$ film was found to effectively shorten the UV light irradiation time required for the surface becoming super-hydrophilicity. Meanwhile, the increase in the film acidity of the SPCE-treated a-TiO$_x$ film due to the fluorine ion incorporation also caused a notable enhancement on the photocatalytic degradation to the cation-rich MB solution, and therefore corresponded a rate constant (~0.0204 min^{-1}) very close to that of the annealed TiO$_x$ film (~0.0258 min^{-1}). By applying such coating to the OLED packaging, the excellent self-cleaning effect (ie. the water contact angle = 0°) was achievable using the internal light (~0.3 mW/cm²) illumination for 7 h. In addition, such an amorphous TiO$_x$ film with nano-textures encapsulated the OLED also was beneficial for enhancing the device's light-extraction efficiency by a factor of about 1.25.

Fig. 8. Photo-induced surface wettability to the water droplet of the controlled OLED, and the OLEDs also encapsulated by the as-deposited and SPCE-treated films, respectively, irradiated by the (a) external UV light and (b) internal blue light.

References

[1] D.S. Liu, T.W. Lin, B.W. Huang, F.S. Juang, P.H. Lei, C.Z. Hu, Appl. Phys. Lett. 94 (2009) 143502.
[2] A.N. Noemaun, F.W. Mont, G.B. Lin, J. Cho, E.F. Schubert, G.B. Kim, C. Sone, J.K. Kim, J. Appl. Phys. 110 (2011) 054510.
[3] X.G. Hou, X.M. Wang, W.J. Luan, D.J. Li, L. Dong, J. Ma, Surf. Coat. Technol. 229 (2013) 71.
[4] Y.L. Fang, X.M. Wang, X.L. Ai, J.G. Huang, Q. Wang, T. Wu, Ceram. Int. 40 (2014) 15941.
[5] J. Zhang, Z.Y. Wu, X. Ju, B.J. Wang, Q.S. Li, T.D. Hu, K. Ibrahim, Y.N. Xie, Opt. Mater. 21 (2003) 573.
[6] S.H. Lee, E. Yamasue, K.N. Ishihara, H. Okumura, Appl. Catal. B 93 (2010) 217.
[7] C.Y. Wu, S.C. Hong, F.T. Hwang, L.W. Lai, T.W. Lin, D.S. Liu, Thin Solid Films 520 (2011) 320.
[8] H.M. Zhang, C.H. Liang, J. Liu, Z.F. Tian, G.Z. Wang, W.P. Cai, Langmuir 28 (2012) 3938.
[9] Z. Lin, Y. Wang, D.N. Wang, B.H. Zhao, J.C. Li, Surf. Coat. Technol. 228 (2013) S131.
[10] M. Nakamura, S. Kato, T. Aoki, L. Sirghi, Y. Hatanaka, J. Appl. Phys. 90 (2001) 3391.
[11] C.Y. Wu, B.S. Chiang, S. Chang, D.S. Liu, Appl. Surf. Sci. 257 (2011) 1893.
[12] H. Kim, W. Choi, Appl. Catal. B 69 (2007) 127.
[13] X.F. Cheng, W.H. Leng, D.P. Liu, Y.M. Xu, J.Q. Zhang, C.N. Cao, J. Phys. Chem. C 112 (2008) 8725.
[14] O. Van Overschelde, G. Guisbiers, F. Hamadi, A. Hemberg, R. Snyders, M. Wautelet, J. Appl. Phys. 104 (2008) 103106.
[15] P.C. Shih, C.H. Huang, T.H. Chen, L.W. Lai, Y.S. Lu, D.S. Liu, Mater. Res. Bull. 52 (2014) 177.
[16] K. Guan, Surf. Coat. Technol. 191 (2005) 155.
[17] H. Park, W. Choi, J. Phys. Chem. B 108 (2004) 4086.
[18] K. Lv, X. Li, K. Deng, J. Sun, X. Li, M. Li, Appl. Catal. B 95 (2010) 383.
[19] L.Y. Liang, Z.M. Liu, H.T. Cao, X.Q. Pan, Appl. Mater. Interfaces 2 (2010) 1060.
[20] A. Vijayabalan, K. Selvam, R. Velmurugan, M. Swaminathan, J. Hazard. Mater. 172 (2009) 914.
[21] H. Li, G. Zhao, G. Han, B. Song, Surf. Coat. Technol. 201 (2007) 7615.
[22] C.T. Hsieh, M.H. Lai, Y.S. Cheng, J. Colloid Interface Sci. 340 (2009) 237.
[23] J. Kim, W. Choi, H. Park, Res. Chem. Intermed. 36 (2010) 127.